Kinetics of Internal Rotation of N,N-Dimethylacetamide: A Spin-Saturation Transfer Experiment

ARTICLE *in* JOURNAL OF CHEMICAL EDUCATION · JULY 1997

Impact Factor: 1.11 · DOI: 10.1021/ed074p978

3 AUTHORS, INCLUDING:

Russell Jarek
Sandia National Laboratories
10 PUBLICATIONS **101** CITATIONS
SEE PROFILE

Seung Koo Shin
Pohang University of Science and Technology
79 PUBLICATIONS **1,347** CITATIONS
SEE PROFILE

Kinetics of Internal Rotation of *N,N*-Dimethylacetamide: A Spin-Saturation Transfer Experiment

An Undergraduate Physical Chemistry Experiment Using FT-NMR To Determine an Internal Rotational Barrier

Russell L. Jarek, Robert J. Flesher, and Seung Koo Shin
Department of Chemistry, University of California, Santa Barbara, Santa Barbara, CA 93106

N,N-Dimethylacetamide (DMA) is a planar molecule with a high rotational barrier about the amide bond due to a partial double-bond character developed in the resonance structure, as shown in Figure 1. The room-temperature ^{1}H-NMR spectrum of DMA as shown in Figure 2 exhibits three sharp methyl peaks. *N*-Methyl-A and -B peaks cis- and trans- to the carbonyl are near 2.6 and 2.2 ppm, respectively, and the *C*-methyl is near 1.6 ppm. As temperature increases, the two *N*-methyl peaks gradually merge into one as the accelerated internal rotation makes them indistinguishable on the NMR detection time scale (*1*). This phenomenon is called a *mutual-site exchange* because each departing group is replaced by an equivalent one. The two exchanging sites are denoted A and B in Figure 1.

Studies of mutual-site exchange kinetics provide the rotational barrier about the amide bond in DMA. The mutual-site exchange kinetics in DMA has been studied in various solvents by line-shape analysis methods (*2–4*). However, the line-shape analysis can be quite complicated and experimentally restrictive. With the strong magnetic fields used today the coalescence temperature exceeds the boiling point of most solvents (*5–6*). In contrast, the spin-saturation transfer method is less restrictive because the experiment can be run in a narrower and lower temperature range and extensive peak fitting is avoided.

Preparation

Instrumentation

The NMR spectrometric features required for this experiment include (i) the pulse programming capability to permit measurement of spin-lattice relaxation times, (ii) a variable temperature probe, and (iii) a pulsed or c.w. decoupler with sufficient selectivity to saturate a single methyl signal from the sample.

Chemical System

The chemical shift difference between the exchanging groups should be sufficient to achieve the selective saturation of the specific *N*-methyl group. However, the partial saturation due to lack of selectivity may be taken into account by monitoring temporal variations of the net magnetizations of the exchanging groups (*7–9*). Choice of solvent may help achieve the selective saturation. For example, DMA in D_2O shows the *N*-methyl peaks separated by only 0.15 ppm, whereas they are separated by 0.45 ppm in toluene-d_8. It is also useful to choose a molecular system that possesses at least one reference peak separated from the exchange sites. The reference peak serves as an internal standard to measure the extent of saturation of the exchange site. With DMA the *C*-methyl peak provides an accurate 1:1 reference.

Students

The students should be familiar with the basic concepts of NMR before proceeding with the experiment. They should be trained in the operation of the spectrometer to the extent that they can acquire and process free-induction-decay signals and carry out an integration to obtain relative peak intensities. (These skills may have been acquired during their organic laboratory course.) The article by Macomber (*11*) discusses Fourier transform NMR (FT-NMR) in a very concise yet thorough manner, and a glossary of NMR terms by King and Williams (*12*) will speed comprehension of the terminology. A series of articles by Rabenstein (*13*), Chesick (*14, 15*), and King and Williams (*16–19*) can be offered as additional reading material for applications of FT-NMR in chemistry. For the spin-lattice relaxation time measurements, the conceptual discussion by Wink (*20*) is helpful. Supplementing the literature with a handout describing usage of the specific NMR and a demonstration should sufficiently prepare students for the experiment.

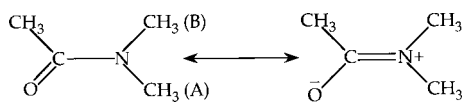

Figure 1. The resonance structure of *N,N*-dimethylacetamide.

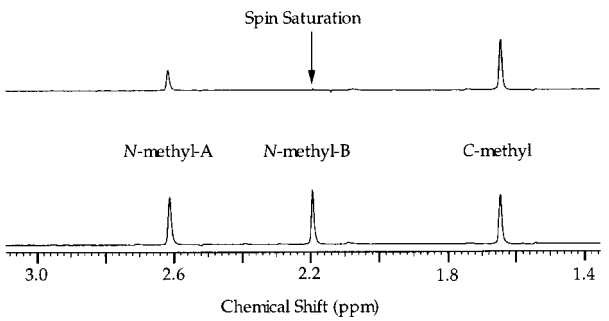

Figure 2. Room temperature ^{1}H-NMR spectrum of DMA in toluene-d_8 with and without decoupler saturation (upper and lower spectrum, respectively). The decrease in the *N*-methyl-A peak is from the spin-saturation transfer process from the *N*-methyl-B peak which is saturated and hence not observed.

Theory

Spin-Saturation Transfer Kinetics

The mutual-site exchange kinetics are shown in Figure 3, where [A] and [A*] are the lower and upper spin-state populations for the methyl-A, and [B] and [B*] are those for the methyl-B, respectively. T_{1A} and T_{1B} are the spin-lattice relaxation times for the methyl-A and B, respectively; k is the mutual-site exchange rate constant.

The rate equations for the lower and upper spin-state populations are considered first in the absence of spin-lattice relaxations as given in eqs 1 and 2 (*7–9*).

$$\frac{d[\mathrm{A}]}{dt} = -k\,[\mathrm{A}] + k\,[\mathrm{B}] = -\frac{d[\mathrm{B}]}{dt} \tag{1}$$

$$\frac{d[\mathrm{A}^*]}{dt} = -k\,[\mathrm{A}^*] + k\,[\mathrm{B}^*] = -\frac{d[\mathrm{B}^*]}{dt} \tag{2}$$

Secondly, spin-lattice relaxation processes that keep spin-state populations in thermal equilibrium are considered in the absence of chemical exchange as expressed in eqs 3 and 4.

$$\frac{dM_\mathrm{A}}{dt} = \frac{M_{0\mathrm{A}} - M_\mathrm{A}}{T_{1\mathrm{A}}} \tag{3}$$

$$\frac{dM_\mathrm{B}}{dt} = \frac{M_{0\mathrm{B}} - M_\mathrm{B}}{T_{1\mathrm{B}}} \tag{4}$$

where $M_\mathrm{A} = [\mathrm{A}] - [\mathrm{A}^*]$ and $M_\mathrm{B} = [\mathrm{B}] - [\mathrm{B}^*]$ are the net magnetizations of the methyl-A and methyl-B, respectively. $M_{0\mathrm{A}}$ and $M_{0\mathrm{B}}$ are the net magnetization of the methyl-A and methyl-B at thermal equilibrium, respectively. Combining eqs 1–4 leads to the rate equations for the net magnetization in the presence of both the chemical exchanges and spin-lattice relaxations as given in eqs 5 and 6.

$$\frac{dM_\mathrm{A}}{dt} = -k\left(M_\mathrm{A} - M_\mathrm{B}\right) + \frac{M_{0\mathrm{A}} - M_\mathrm{A}}{T_{1\mathrm{A}}} \tag{5}$$

$$\frac{dM_\mathrm{B}}{dt} = k\left(M_\mathrm{A} - M_\mathrm{B}\right) + \frac{M_{0\mathrm{B}} - M_\mathrm{B}}{T_{1\mathrm{B}}} \tag{6}$$

The rate equations may be simplified by taking $T_{1\mathrm{A}} = T_{1\mathrm{B}}$ ($= T_1$), which is a good approximation for the *N*-methyl protons in DMA. The sum, $M_\mathrm{A} + M_\mathrm{B}$, and difference, $M_\mathrm{A} - M_\mathrm{B}$, of eqs 5 and 6 yield the first-order rate equations 7 and 8.

$$\frac{d}{dt}\left(M_\mathrm{A} + M_\mathrm{B}\right) = \frac{M_{0\mathrm{A}} + M_{0\mathrm{B}} - M_\mathrm{A} - M_\mathrm{B}}{T_1} \tag{7}$$

$$\frac{d}{dt}\left(M_\mathrm{A} - M_\mathrm{B}\right) = -\left(2k + \frac{1}{T_1}\right)\left(M_\mathrm{A} - M_\mathrm{B}\right) \tag{8}$$

Solutions of eqs 7 and 8 are given in eqs 9 and 10.

$$M_\mathrm{A}(t) + M_\mathrm{B}(t) - M_{0\mathrm{A}} - M_{0\mathrm{B}} = \left[M_\mathrm{A}(0) + M_\mathrm{B}(0) - M_{0\mathrm{A}} - M_{0\mathrm{B}}\right]\exp^{-t/T_1} \tag{9}$$

$$M_\mathrm{A}(t) - M_\mathrm{B}(t) = \left[M_\mathrm{A}(0) - M_\mathrm{B}(0)\right]\exp^{-\left(2k + 1/T_1\right)t} \tag{10}$$

These solutions are quite general and applicable to the spin-population recovery kinetics with any initial values of $M_\mathrm{A}(0)$ and $M_\mathrm{B}(0)$. Temporal variations of the sum and difference magnetizations can be fit to eqs 9 and 10 to obtain both T_1 and k.

The selective spin saturation of the methyl-B, also shown in Figure 2, is most conveniently done with a spectrometer decoupler. With a sufficiently long duration of decoupler r.f. pulse, the spin states of the methyl-B can be saturated to have equal populations in the upper and lower spin states, that is, $M_\mathrm{B} = [\mathrm{B}] - [\mathrm{B}^*] = 0$. This spin-state saturation makes the methyl-B peak disappear from the spectrum when a 90° probe pulse is applied to monitor the net magnetization (signal intensity) after saturation. Over time, the saturated spin population is transferred to the methyl-A via internal rotation, resulting in partial loss of net magnetization of the methyl-A from its thermal equilibrium value, $M_{0\mathrm{A}}$, observed in the absence of saturation. If the spin saturation of the methyl-B is prolonged for M_A to reach the steady state, that is, $dM_\mathrm{A}/dt = 0$ and $M_\mathrm{B} = 0$, then eq 5 can be used directly to determine the rate constant for the spin-saturation transfer.

$$k = \frac{1}{T_{1\mathrm{A}}}\left(\frac{M_{0\mathrm{A}}}{M_\mathrm{A}} - 1\right) \tag{11}$$

The spin-relaxation times, $T_{1\mathrm{A}}$ and $T_{1\mathrm{B}}$, can be obtained from the separate inversion recovery experiments.

Thermodynamics

Since the internal rotation about the amide bond is an equilibrium process, the absolute rate theory can be used to evaluate activation parameters involved in the process. The rate of mutual site-exchange can be expressed with the Eyring equation (eq 12) or with the Arrhenius equation (eq 13) (*1, 10*).

$$k = \kappa\frac{k_\mathrm{B}T}{h}\exp^{-\Delta G^\ddagger/RT} \tag{12}$$

$$k = A\exp^{-E_a^\ddagger/RT} \tag{13}$$

Here, κ is the transmission coefficient—that is, the fraction of the reactant reaching the transition state that proceeds to the product; k_B is the Boltzmann constant; h is the Planck constant; $\Delta G^\ddagger$ is the free energy of activation; and R is the gas constant. A is the preexponential factor and $E_a^\ddagger$ is the activation energy. Both the enthalpy ($\Delta H^\ddagger$) and entropy ($\Delta S^\ddagger$) of activation can be determined from the plot of ln ($k\,T^{-1}$) vs. T^{-1} using eq 14 with $\kappa = 1$.

$$\ln\left(\frac{k}{T}\right) = \ln\left(\frac{k_B}{h}\right) - \frac{\Delta H^\ddagger}{RT} + \frac{\Delta S^\ddagger}{R} \tag{14}$$

Arrhenius' parameters at a given temperature are related to $\Delta H^\ddagger$ and $\Delta S^\ddagger$.

$$E_a = \Delta H^\ddagger + RT \tag{15}$$

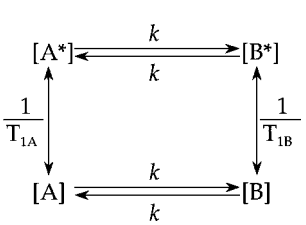

Figure 3. Scheme for two-site exchange kinetics. [A] and [A*] are the lower and upper spin-state populations for the methyl-A and [B] and [B*] are those for the methyl-B, respectively. k is the rate constant for the internal rotation and T_1 is the spin-lattice relaxation time.

Table 1. Experimental Data for Spin-Saturation Transfer Kinetics Measurement

T (°C)	M_A/M_{0A}	Measured T_1 (s)	k (s^{-1})
5.0	0.734 (.015)	4.14 (.09)	0.087 (.003)
10.0	0.583 (.008)	4.28 (.10)	0.167 (.005)
12.5	0.531 (.002)	4.24 (.22)	0.208 (.011)
15.0	0.430 (.001)	4.48 (.14)	0.289 (.009)
17.5	0.392 (.002)	4.66 (.13)	0.333 (.009)
20.0	0.326 (.004)	4.63 (.12)	0.447 (.013)
22.5	0.254 (.005)	4.73 (.14)	0.608 (.022)

$$\ln A = \frac{\Delta S^{\ddagger}}{R} + \ln\left(\frac{ek_B T}{h}\right) \qquad (16)$$

An RT term in eq 15 results from one vibrational degree of freedom in the low-frequency torsional mode lost in the transition state.

Experimental Procedures

Sample Preparation

A dilute solution of analytic grade *N*,*N*-dimethylacetamide in toluene-d_8 was prepared in a standard 5-mm NMR sample tube in the presence of air. Both reagents were purchased from Aldrich Chemical Co. Since the activation parameters are concentration-dependent (*2*), it is advisable to use the same sample for the entire experiment. The probe temperature reading was calibrated at each temperature with neat methanol or glycol (*21*) following the automated calibration procedures outlined in the operating instructions. The temperature calibration curve was measured once and used by the entire class.

Data Acquisition

A Varian Gemini 200 MHz NMR spectrometer was employed in our experiment. A series of spectra at seven different temperatures was acquired for the derivation of activation parameters. In a 200-MHz NMR the useful temperature range for DMA in toluene-d_8 is 0–25 °C. First, the NMR probe was set idle for 10–15 min to establish thermal equilibrium at each temperature and the magnet was shimmed as necessary. Line widths on the order of 1 Hz were readily obtained and were adequate for the purposes of the experiment. Carrier frequency, sweep width, and data block size were set to provide a digital resolution of at least 0.3 Hz/point in the spectrum. A quick spectrum was taken to check the sample purity and to define the peak positions for integration.[1]

To initiate the kinetics measurements. the spin-lattice relaxation times were measured by the inversion recovery method[2] (*18*, *20*), taking ca. 15 min at each temperature. For the spin-saturation transfer experiment, the spin-decoupler power level and pulse duration were adjusted to remove the irradiated *N*-methyl peak from the spectrum while not affecting the other *N*-methyl signal.[3] *N*-Methyl-B trans- to the carbonyl (near 2.2 ppm) was saturated in our experiment. After finding a suitable decoupler level, the degree of decoupling overlap was tested by shifting the decoupler position to ca. 3.0 ppm (ca. 0.4 ppm downfield from *N*-methyl-A near 2.6 ppm). The spectrum taken at the new decoupler position showed three methyl peaks with equal integrated intensities, indicating that the irradiation at the *N*-methyl-B does not directly affect the intensity of the nearest neighbor peak of *N*-methyl-A ca. 0.4 ppm upfield. Thus, the intensity changes of the *N*-methyl-A peak observed from the spin decoupling of the *N*-methyl-B peak must arise from the mutual-site exchange.

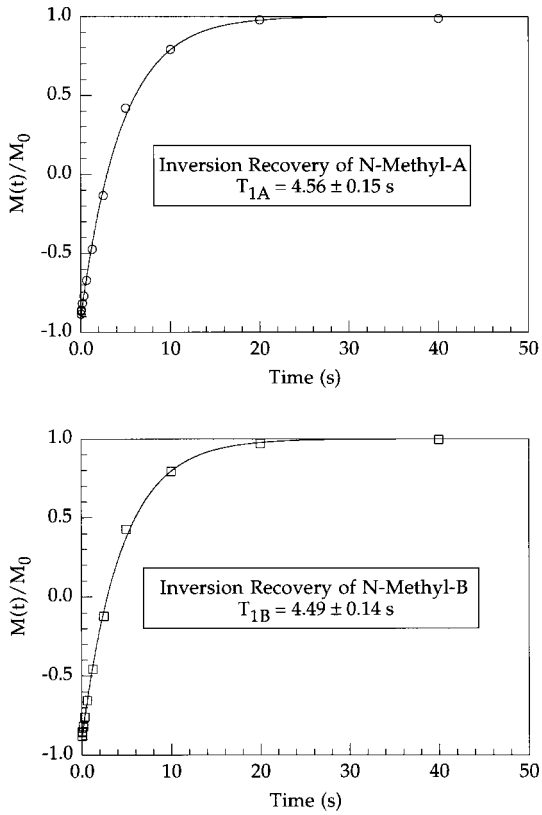

Figure 4. Inversion recovery data at 15 °C with fitting to integrals of eqs 3 and 4. As assumed, $T_{1A} = T_{1B}$ within the experimental error.

The mutual-site exchange spectrum was obtained at several probe temperatures with the spin decoupler applied on resonance with the *N*-methyl-B peak for a period of at least $5T_1$ before the probe pulse. The *N*-methyl-A and *C*-methyl peaks were integrated to obtain values for M_A and M_{0A}, respectively. An average peak ratio and the standard deviation were calculated by taking several spectra under identical conditions to complete the kinetics measurements.

Results and Discussion

The room-temperature ^{1}H-NMR and spin-saturation transfer spectra of DMA are shown in Figure 2. The ratio of the *N*-methyl-A to the *C*-methyl peaks, M_A/M_{0A} ($M_{0A} = M_C$) (Table 1), is obtained from the integrated intensities. Nuclear Overhauser effects were absent.

Figure 4 shows the data for the inversion recovery kinetics at 15 °C and fits to the integrals of eqs 3 and 4. The spin-lattice relaxation times for the *N*-methyl-A and *N*-methyl-B peaks are obtained as 4.56 ± 0.15 and 4.49 ± 0.14 s, respectively. The two *N*-methyl groups have almost identical T_1 within experimental uncertainties, which substantiates the assumption of $T_{1A} = T_{1B}$. The temperature dependence of T_1 for the *N*-methyl-A is plotted in Figure 5 in the temperature range 5–22.5 °C. The thermal variation of T_1

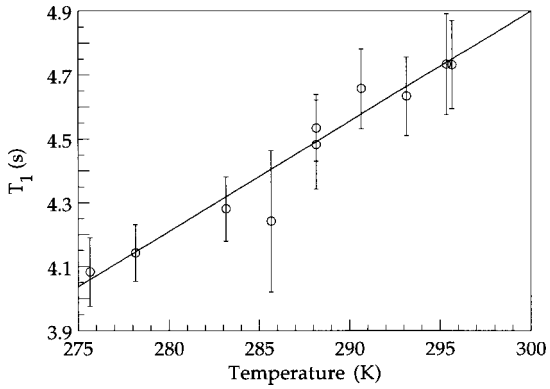

Figure 5. The temperature dependence of the spin-lattice relaxation time of the *N*-methyl-A cis- to the carbonyl at 2.6 ppm.

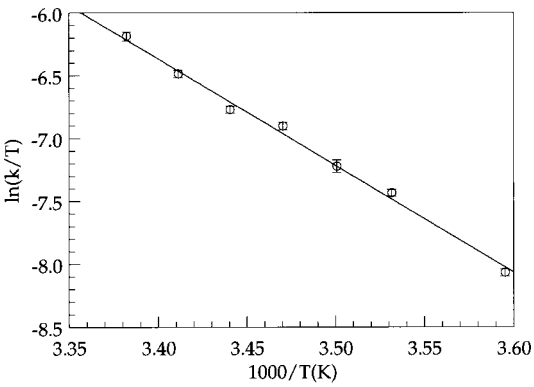

Figure 6. Plot of ln ($k\ T^{-1}$) as a function of T^{-1}. Slope and intercept values are used in eq 14 to determine the enthalpy and entropy of activation.

necessitates its determination at each temperature.

The rate constant for the internal rotation is calculated using eq 11 at each temperature. Experimental data are listed in Table 1. Values in parenthesis represent experimental errors of the measurement. A plot of ln ($k\ T^{-1}$) vs. T^{-1} is shown in Figure 6. Error bars represent experimental errors propagated to the rate constant calculations. The temperature uncertainty on the probe was 0.5 K. An error-weighted least-squares fit gives thermodynamic parameters for internal rotation with eq 14. The slope and intercept of the plot in Figure 6 yield $\Delta H^{\ddagger}_{298} = 70.6 \pm 1.4$ kJ mol^{-1} and $\Delta S^{\ddagger}_{298} = -10.5 \pm 5.0$ J mol^{-1} K^{-1}. The Gibbs free energy and Arrhenius's activation parameters are evaluated from the enthalpy and entropy of activation. They are $\Delta G^{\ddagger}_{298} = 73.7 \pm 2.0$ kJ mol^{-1}, $E_a = 73.1 \pm 1.4$ kJ mol^{-1}, and $A = (4.8 \pm 2.3)\ 10^{12}$ s^{-1}. Table 2 compares these activation parameters with those reported from the line-shape analyses. Note that $\Delta S^{\ddagger}_{298}$ or A is notoriously hard to measure by NMR methods. The present results are in good agreement with the reported values derived from the different solvent systems. It appears that the activation energy of internal rotation increases with increasing dipole moment of solvent. The present activation parameters are bracketed by the nonpolar CCl_4 and polar D_2O solvents.

The activation energy obtained from the spin-saturation transfer kinetics is useful in the visualization of the amplitude of internal rotation. The potential function for the torsional vibration with the rotational symmetry of 2 is given in eq 17 as a function of torsional angle, ϕ (*23*).

$$V(\phi) = \frac{V}{2}\left(1 - \cos 2\phi\right) \qquad (17)$$

An angle $\phi = 0$ denotes a planar structure. The height of the potential, $V = 71.7$ kJ mol^{-1}, is the sum of the activation energy at 0 K (70.6 kJ mol^{-1}) and the zero-point energy of torsional vibration (1.11 kJ mol^{-1}). The torsional frequency of DMA is 186 cm^{-1} (*24*). The zero-point energy level corresponds to a torsional angle $\phi = 7.2°$ in eq 17, which represents the angular displacement of the internal rotation about the amide bond in DMA at 0 K.

In summary, the spin-saturation transfer kinetics measurement was performed to probe the internal rotation of *N*,*N*-dimethylacetamide in toluene-d_8. Though the temperature range is narrow compared with the line-shape analysis experiment, the derived thermodynamic data are in excellent agreement with more extensive measurements. This experiment has been tested for three years and successfully adopted in our undergraduate physical chemistry laboratory.

Table 2. Activation Parameters for the Internal Rotation of *N*,*N*-Dimethylacetamide

Parameter	Reference				
	This Work	*2*	*3*	*3*	*3*
E_a (kJ mol^{-1})	73.1±1.4	70.5±1.7	82.8±0.4	82.0±1.3	79.5±0.4
$\Delta G^{\ddagger}_{298}$ (kJ mol^{-1})	73.7±2.0	72.5	80.8±0.4	75.3±0.4	75.7±0.4
$\Delta H^{\ddagger}$ (kJ mol^{-1})	70.6±1.4	68.0	79.9±0.4	79.5±1.3	76.6±0.4
$\Delta S^{\ddagger}$ (J mol^{-1} K^{-1})	-10.5±5.0	-15.0±5.1	-3.3±4.2	13±8	2.9±4.2
Solvent	Toluene-d_8	CCl_4	D_2O	Acetone-d_6	Neat DMA
Method	Spin-saturation transfer	Line-shape analysis	Line-shape analysis	Line-shape analysis	Line-shape analysis
μ (Debye)[a]	0.36	0.00	1.85	2.88	3.81

[a]Dipole moments for the solvents are taken from ref *22*.

Acknowledgment

S.K.S. thanks J. T. Gerig and M. DiMare for helpful discussions of the experiment and manuscript. The authors also thank Ata Shirazi for his help in operating a variable-temperature Varian GEMINI-200 NMR spectrometer. S.K.S. acknowledges support from the National Science Foundation-Young Investigator Award under Grant No. CHE-9457668. The Varian GEMINI-200 NMR spectrometer was partly supported by the NSF 90-101 Instrumentation and Laboratory Improvement Program under Grant No. USE-9151415.

Notes

1. Typical Gemini 200 commands are outlined. Enter SU to adjust the setup parameters and GA to acquire and process the free-induction-decay (FID).

2. Enter DOT1 to set up the inversion recovery pulse sequence for the T_1 measurement. The program asks the user to type in values for the approximate minimum and maximum T_1 and the length of time to run. Enter DT1 to obtain numerical results.

3. Move the cursor on the peak to be decoupled and enter SDA (Set Decoupler Array). Then change to decoupler mode by entering DG followed by entering DM=Y. Also set HOMO=Y for homonuclear decoupling. To set the decoupler power level, enter DLP=# (#=0 – 2048). Our typical # was 1800.

Literature Cited

1. Abraham, R. J.; Loftus, P. *Proton and Carbon-13 NMR Spectroscopy*; Heyden: London, 1978.
2. Reeves, L.; Shaddick, R.; Shaw, K. *Can. J. Chem.* **1971,** *49*, 3683–3691.
3. Drakenberg, T.; Dahlqvist, K.; Forsen, S. *J. Phys. Chem*. **1972,** *76*, 2178–2183.
4. Fujiwara, F.; Airoldi, C. *J. Phys. Chem.* **1984,** *88*, 1640–1642.
5. Sandstrom, J. *Dynamic NMR Spectroscopy*; Academic: New York, 1982.
6. Harris, R. K. *Nuclear Magnetic Resonance Spectroscopy*; Pitman: London, 1983.
7. McConnell, H. M. *J. Chem. Phys*. **1958,** *28*, 430.
8. Ugurbil, K. *J. Magn. Reson.* **1985,** *64*, 207–219.
9. Bellon, S. F.; Chen, D.; Johnston, E. R. *J. Magn. Reson*. **1987,** *73*, 168–173.
10. Glasstone, S.; Laidler, K. J.; Eyring, H. *The Theory of Rate Processes*; McGraw-Hill: New York, 1941.
11. Macomber, R. *J. Chem. Educ.* **1985,** *62*, 213–214.
12. King, R.; Williams, K. *J. Chem. Educ.* **1990,** *67*, A100–A104.
13. Rabenstein, D. L. *J. Chem. Educ.* **1984,** *61*, 909–913.
14. Chesick, J. P. *J. Chem. Educ*. **1989,** *66*, 128–132.
15. Chesick, J. P. *J. Chem. Educ.* **1989,** *66*, 283–289.
16. King, R.; Williams, K. *J. Chem. Educ.* **1989,** *66*, A213–A219.
17. King, R.; Williams, K. *J. Chem. Educ.* **1989,** *66*, A243–A248.
18. Williams, K.; King, R. *J. Chem. Educ.* **1990,** *67*, A93–A99.
19. Williams, K.; King. R. *J. Chem. Educ.* **1990,** *67*, A125–A137.
20. Wink, D. *J. Chem. Educ.* **1989,** *66*, 810–813.
21. Van Geet, A. L. *Anal. Chem*. **1968,** *40*, 2227–2229.
22. *CRC Handbook of Chemistry and Physics*; Weast, R. C., Ed.; CRC: Boca Raton, FL; pp E59–E61.
23. Lister, D. G.; Macdonald, J. N.; Owen, N. L. *Internal Rotation and Inversion*; Academic: London, 1978.
24. Dwivedi, A. M.; Krimm, S.; Mierson, S. *Spectrochim. Acta* **1989,** *45A*, 271–279.